Available online at www.sciencedirect.com
SCIENCE DIRECT®
ELSEVIER
International Journal of Multiphase Flow 30 (2004) 1121–1138
International Journal of Multiphase Flow
www.elsevier.com/locate/ijmulflow

Experimental investigation of interparticle collision rate in particulate flow

Changfu You *, Hailiang Zhao, Yi Cai, Haiying Qi, Xuchang Xu

State Key Laboratory of Clean Combustion of Coal, Tsinghua University, Beijing 100084, PR China

Received 17 December 2003; received in revised form 2 May 2004

Abstract

Interparticle collision is an important phenomenon in the mechanics of two-phase flow. Most past researches on this problem have been based on the analogy with kinetic theory of gases with few experimental validations of the results. While this paper presents the directly measured experimental data of collision rate in vertical two-phase flow. This research used a high-speed camera and Particle Tracking Velocimetry (PTV) algorithms to focus on the interparticle collisions, especially the collision rate, on a millisecond time scale and a millimeter space scale, which is the particle size (1.8 mm in diameter). The camera speed was normally 2000 frames per second with an exposure of 1/2000 s and a laser power of 25 W for particle velocity of less than 4m/s in the collision region and particle fractions of about 0.015. A manual count of the collision numbers was chosen as the most accurate method for the determination of the collision rate. The PTV algorithms were applied to calculate the particle number density and relative velocities. The correlation between the particle collision rate, the particle number density, the average relative velocity between particles and the measured granular temperature, was compared with commonly used relations based on kinetic theory. The results demonstrated that great differences exist between the theoretical and experimental results for these experimental conditions. The collision rate determined experimentally is much lower than the theoretical estimation based on kinetic theory. This means the theoretical correlations overestimate the collision rate in the gas-particle flows. This discrepancy may be attributed to the assumptions in the theoretical collision model and experimental error.

Keywords: Interparticle collision; Collision rate; Collision frequency; PTV; Two-phase flow; Gas-particle flow

* Corresponding author. Tel./fax: +86-10-6278-1740.
E-mail address: youcf@tsinghua.edu.cn (C. You).

0301-9322/$ - see front matter
doi:10.1016/j.ijmultiphaseflow.2004.05.009

1. Introduction

Interparticle collisions play a significant role in numerical simulations and theoretical analyses of real gas-particle two-phase flows, such as pneumatic conveying, fluidized beds, mixing devices and others. In such particle-laden flows the particle behaviors may be considerably affected by interparticle collisions in addition to aerodynamic transport and turbulent effects if the mass loading is high or regions of high concentration developed as a result of inertial effects (Sommerfeld, 1995). In this condition, the effect of collisions between particles is no longer negligible (Crowe, 1981) even at particle volume fractions as low as 4×10^{-4} (Tanaka and Tsuji, 1991). To improve our understanding of such collision flows, the collisions between particles have been studied numerically using various models, either an Eulerian approach where each phase is considered as a continuum fluid or a Lagrangian approach where representative particle trajectories are computed. Early Lagrangian calculations dealt with dilute flows (for example Matsumoto and Saito, 1970a,b) where only particle–wall interactions were considered. Thanks to the continuous and rapid growth of computer capacities, Lagrangian simulations of more complex flows with consideration of interparticle collisions have become possible. Two approaches can be used to account for the interparticle collisions in the frame of the Euler/Lagrange method for the numerical calculation of two-phase flows. The first method consists in simultaneously computing the trajectories of all the particles in the flow domain, thus making it possible to handle the collisions in a deterministic way (Ottjes, 1978; Tsuji et al., 1990; Tanaka and Tsuji, 1991). However, the huge number of particles in actual flows and the very small time interval, which must be used, limit this method to relatively small problems, if one wants to preserve reasonable computation times. More recently, a second method proposed by several authors (Tanaka and Tsuji, 1991; Oesterle and Petitjean, 1991, 1993; Sommerfeld and Zivkovic, 1992; Sommerfeld, 2001) has used a Monte Carlo type Lagrangian simulation technique, which includes computation of only a restricted number of trajectories with interparticle collisions analyzed by means of a probabilistic collision model.

However, this collision model is derived according to the analogy of kinetic theory of gases. Such probabilistic models need to be tested (Sommerfeld, 1994) by measurements of a suspension flow where collisions between particles play an important role. Any improvement of the predictions will also surely require a better knowledge of the parameters governing the particle-to-particle collision process such as the collision frequency. This could be achieved by directly measuring the distribution of the collision frequency on a vertical channel facility (Fohanno and Oesterle, 2000).

This is the goal of the present study, which aims to provide direct experimental data on the collisions of large particles in a particular flow configuration where the effects of interparticle collisions are significant. This is significant to the validation of the theoretical collision models derived from kinetic theory.

2. Interparticle collision rate

Firstly, some quantities used in the analysis of particle collisions need to be defined clearly. In a particulate system, interparticle collision rate N_c is defined as the total number of interparticle

collisions per unit time per unit volume, and the collision frequency f_c is defined as the number of collisions undergone by one single particle per unit time. The relation between them is

$$N_c = \frac{1}{2} n f_c \tag{1}$$

where n is the particle number density and the factor 1/2 is a correct for the double counting between identical particles.

A useful theory of interparticle collisions would predict the average collision rate from known properties of the flow and the particle phase (e.g. concentration, diameter, and density.) Quite a number of theoretical studies on the collision rate of particles or droplets in turbulent flows have been published in the past. A detailed review was given for example by Williams and Crane (1983) and Pearson et al. (1984).

The consideration of interparticle collisions in the most commonly applied Lagrangian approach where one particle is tracked after the other through the flow field requires the derivation of an appropriate collision model, since no information is available about neighboring particles. Recently, Sommerfeld and Zivkovic (1992) and Oesterle and Petitjean (1993) developed independently a similar probabilistic interparticle collision model, which was based on the calculation of the collision probability along the particle trajectory in analogy with kinetic theory of gases. In these models collision frequency is the key quantity for the calculation of collision probability.

Collision frequency relations have been derived using kinetic theory, for example the derivation given by Bird (1994). First assume the domain has only two classes of particles with different diameters and concentrations, particles A and B. Their diameters are d_1, d_2 and their concentrations are n_1, n_2, with an equivalent diameter $d = (d_1 + d_2)/2$, then the effective collision area as shown in Fig. 1 is:

$$S = \pi d^2 \tag{2}$$

If the velocity of particle A is $\overrightarrow{v_i}$ and that of B is $\overrightarrow{v_j}$, then the relative velocity between A and B is $\overrightarrow{v_r} = \overrightarrow{v_i} - \overrightarrow{v_j}$. Now choose a reference frame in which particle A moves with velocity $\overrightarrow{v_r}$ while particle class B is stationary. Then, over a time interval Δt, particle A would collide with any particle B that has its center within the cylinder of volume $|\overrightarrow{v_r}|\Delta t S$, as shown in Fig. 2.

The collision frequency of a single particle of class A (i.e. $n_1 = 1$) with all other particles in class B is, therefore,

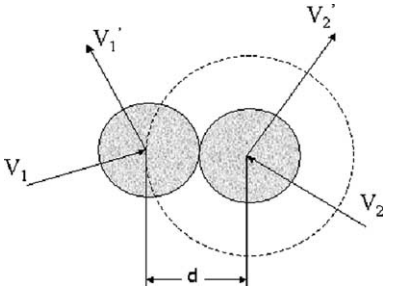

Fig. 1. Equivalent diameter.

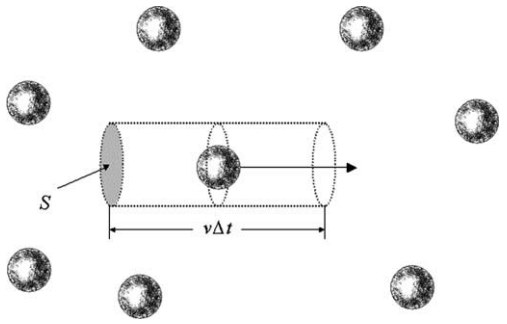

Fig. 2. Effective collision volume swept out by moving particle A among stationary particles B.

$$f_c = \pi d^2 n_2 \overline{v_{ri}} \tag{3}$$

In Eq. (3), $\overline{v_{ri}}$, defined as $\overline{v_{ri}} = \frac{1}{N_j}\sum_{j=1}^{N_j} |\overrightarrow{v_i} - \overrightarrow{v_j}|$ $(j \neq i)$, is the average relative velocity of the considered particle i with all other particles in class B. N_j is the total particle number of class B in the investigation volume. Considering the number density of A class particles, the total number of collisions of particle A with all other particles B per unit time per unit volume is:

$$N_{ci} = \pi d^2 n_1 n_2 \overline{v_r} \tag{4}$$

In Eq. (4), $\overline{v_r}$, defined as $\overline{v_r} = \frac{1}{N_i N_j}\sum_{i=1}^{N_i}\sum_{j=1}^{N_j} |\overrightarrow{v_i} - \overrightarrow{v_j}|$ $(j \neq i)$, is the average relative velocity between all particles in the investigation volume. In a monodisperse particulate system, the total number of collisions per unit time per unit volume (collision rate) is:

$$N_c = \frac{1}{2}\pi d^2 n^2 \overline{v_r} \tag{5}$$

where the factor 1/2 is included to correct for double counting of collisions between identical particles. This shows that the collision rate is a function of particle diameter, particle number density and their average relative velocity.

Also, the derivation of Sundaram and Collins (1997) gave the same expression. Consider a system of N_p particles of diameter d in a volume V. From a development analogous to kinetic theory of gases, the average collision rate N_c in such a monodisperse particulate system can be expressed as:

$$N_c = \frac{1}{2}\pi d^2 n^2 \overline{v_r} g(d) \tag{6}$$

where n is the particle number density and $\overline{v_r}$ is the average relative particle velocity. $g(d)$ is the particle radial distribution function at contact, related to the probability density function of the relative particle separation. It represents a correction to the local number density due to non-uniformities in the spatial particle distribution. As particle position is random and the particle volume fraction is small, $g(d) \approx 1$. So the same expression of collision rate is obtained:

$$N_c = \frac{1}{2}\pi d^2 n^2 \overline{v_r} \tag{7}$$

The collision models of Sommerfeld and Zivkovic (1992) and Oesterle and Petitjean (1993) independently gave the collision frequency to be:

$$f_c = \sqrt{2}\pi(R_1 + R_0)^2|\overrightarrow{v_1} - \langle\overrightarrow{v_0}\rangle|n \quad \text{(by Oesterle and Petitjean, 1993)} \tag{8}$$

$$f_c = \pi(R_1 + R_0)^2|\overrightarrow{v_1} - \langle\overrightarrow{v_0}\rangle|n \quad \text{(by Sommerfeld and Zivkovic, 1992)} \tag{9}$$

where v_0 and R_0 are the velocity and radius of the environmental particle (Oesterle and Petitjean) or fictitious particle (Sommerfeld and Zivkovic) defined in their research, which represents the mean properties of the particles surrounding the particle tracked using the Lagrangian approach, n is the particle number per unit control volume, i.e. the particle number density. These two expressions are nearly the same, except that Eq. (8) includes a factor $\sqrt{2}$ accounting for the difference between the one-dimensional situation and the three-dimensional one, with the assumption of a Maxwellian distribution of the particle relative velocity with respect to the local average solid phase velocity.

Referring to the surrounding particle property defined by Oesterle and Petitjean (1993) or the fictitious particle concept by Sommerfeld and Zivkovic (1992), the average relative velocity $\overline{v_r}$ is similarly defined as:

$$\overline{v_{ri}} = \frac{1}{N_j}\sum_{j=1}^{N_j}|\overrightarrow{v_i} - \overrightarrow{v_j}| \ (j \neq i) \tag{10}$$

$$\overline{v_r} = \frac{1}{N_i}\sum_{i=1}^{N_i}\overline{v_{ri}} \tag{11}$$

The analysis above suggests a general relation for the collision frequency of a single particle and collision rate from the analogy with kinetic theory of gases:

$$f_c = \alpha\pi d^2\overline{v_r}n \tag{12}$$

$$N_c = \frac{1}{2}\alpha\pi d^2\overline{v_r}n^2 \tag{13}$$

where α is a coefficients which equals $\sqrt{2}$ in Eq. (8) (by Oesterle and Petitjean, 1993) and 1 in Eq. (9) (by Sommerfeld and Zivkovic, 1992). It is shown that the number of collisions undergone by a particle is proportional to the number density of the surrounding particles, while the total number of collisions in the disperse phase is proportional to the square of the particle number density.

The granular temperature can also be used to express the collision rate in particle kinetic theory (Gidaspow, 1994), which is usually used in the Eulerian approach for simulating two-phase flow. Based on limited experimental measurements of instantaneous velocities of particles in a liquid fluidized bed by Carlos and Richardson (1968), the particle velocity distribution can be assumed to follow a normal distribution about its mean value $\vec{u}$, which can be defined in terms of the instantaneous velocity $\vec{v}$:

$$\vec{u} = \langle\vec{v}\rangle \tag{14}$$

The fluctuating velocity $\vec{v}'$ about the mean value can be defined as:

$$\vec{v}' = \vec{v} - \vec{u} \tag{15}$$

Then, the granular temperature is:

$$\Theta = \frac{1}{3}\langle|\vec{v}'|^2\rangle \tag{16}$$

In granular flows with two classes of particles having diameters d_1 and d_2, Gidaspow (1994) gave the number of binary collisions per unit time per unit volume as:

$$N_{12} = 4n_1 n_2 d^2 g_0 \sqrt{\pi\Theta} \tag{17}$$

where n_1 and n_2 are the particle number densities, and d is the effective collision diameter. g_0 is a function of the solid volume fraction ε in the flow:

$$g_0(\varepsilon_s) = \left[1 - \left(\frac{\varepsilon_s}{\varepsilon_{s\max}}\right)^{1/3}\right]^{-1} \tag{18}$$

For particles with the same diameter d, Eq. (17) becomes:

$$N_c = 4\sqrt{\pi} n^2 d^2 g_0 \sqrt{\Theta} \tag{19}$$

As pointed by Sommerfeld (1994) and Fohanno and Oesterle (2000), these collision models need validation by direct measurements in suspension flow in which particle collisions are prevailing. However, no experimental data from real gas-particle two-phase flows is available. The current project seeks obtaining experimental data to test these models. In real experimental tests, a single moving particle cannot be easily tracked and the collision frequency is even more difficult to measure. Therefore, the tests in this stage sought to investigate the total collision number per unit time per unit volume, N_c. Considering an investigation volume in the flow field, the total inter-particle collision number in the volume ΔV during time interval Δt can be measured as C. Therefore,

$$N_c = \frac{C}{\Delta V \Delta t} \tag{20}$$

In the present research, an experimental rig was designed, which could be used to specially perform the collision process and then record sequential images by a high-speed camera. The images were processed by Particle Tracking Velocimeter (PTV) algorithms to identify the particle velocities. The experimental results were then used to validate the theoretical collision rate models given by Eqs. (13) and (19).

3. Experimental setup and methods

3.1. Experimental setup

The collision rate was measured in an experimental rig that was based on Fohanno and Oesterle's (2000) experimental setup. The experimental system illustrated in Fig. 3 includes three parts: a particle feeder with a vertical duct, a vertical duct with a convergent particle outlet and a rectangular cross-section larger than that used in the particle feeder, and a photographic equipment. The same flow configuration conceived by Fohanno and Oesterle's (2000) was utilized to

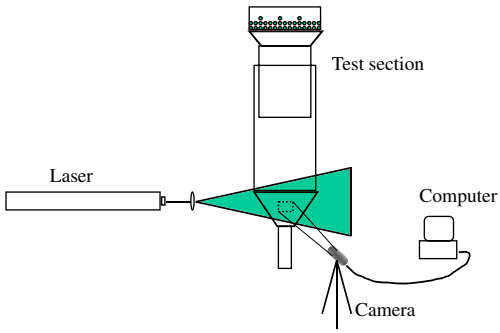

Fig. 3. Experimental setup of the visualization of interparticle collisions.

create a collisional flow, but the photographic technology and image processing methods were different.

The flow was chosen so that the effect of the particle collisions would be significant. The flow geometry was a vertical convergent channel with a rectangular cross-section. The channel was made of glass to enable the optical flow measurements. The duct dimensions are given in Fig. 4. The particle feeder was located above the top section of the duct and could be moved up and down to change the particle velocities into the collision region. The feeder was a container where particles were stored before being released into the channel through a rectangular movable steel

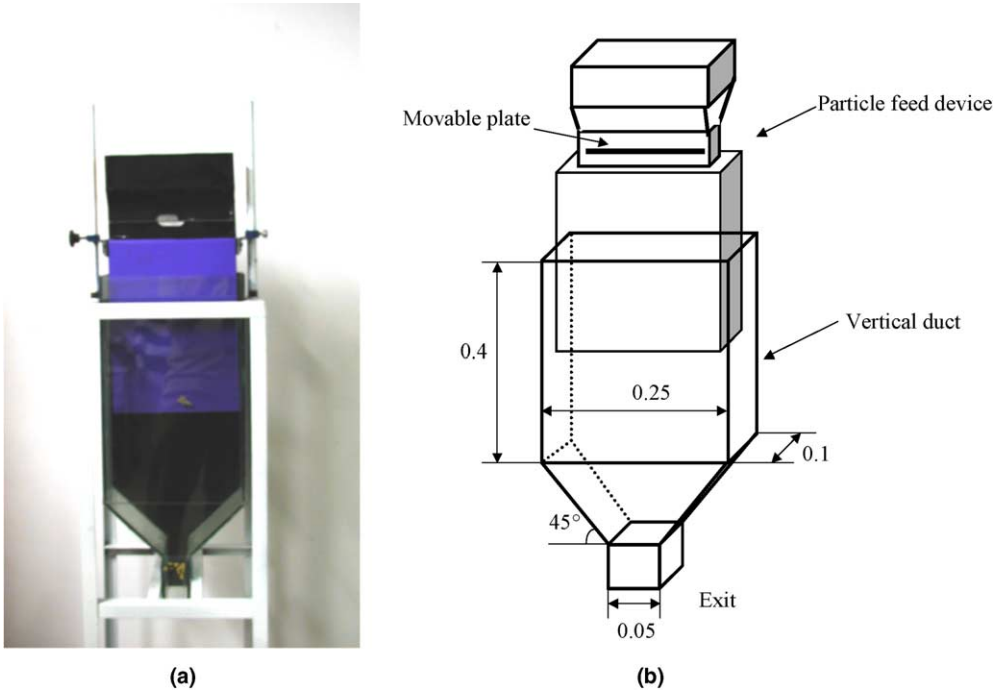

Fig. 4. Duct geometry: (a) photograph and (b) schematic dimensions.

plate. The particle inlet was made as a very thin and long gap in order to confine the flow as two-dimensional phenomenon.

The particles initially fell from the feeder without any collisions between them or with the walls under the sole effect of gravity, the surrounding fluid (air) being initially at rest. During their free fall, the particles accelerated a velocity of about 3.5 m/s. Some particles then reached the convergent section having two sidewalls inclined at 45° with the vertical, which caused numerous particle–wall collisions. Trajectories of colliding particles were then modified and the resulting crossing of the oblique trajectories with those of particles, which were still falling vertically, resulting in collisions between particles. The collisions were then visualized using a high-speed camera.

The main difference between our setup and that of Fohanno and Oesterle (2000) was the optical visualization method. They used a regular film camera to record still photographs that were analyzed using particle streak velocimetry (PSV), with a halogen spotlight to illuminate the channel. The current experiments used a high-power laser sheet as an illumination device, a high-speed CCD camera as image recorder, as well as PTV technique used for the image analysis. The laser was an Argon Ion Laser Continuous Beam System (BEAMLOK 2080-25S, Spectra-Physics Ltd.). The high-speed camera had a maximum speed of 10,000 fps (FASTCAM Super 10 K, Photron Ltd.) to record the images of the particle collisions. The camera speed was normally 2000 fps with an exposure of 1/2000 s and a laser power of 25 W for particle velocities of less than 4 m/s in the collision region and particle fractions of about 0.015.

Various experimental parameters were varied in the tests. The particle velocity was varied by changing the height of the particle feeder. The particle concentration, n, was varied by changing the particle inlet section. The particle diameter distribution was uniform with $d_p = 1.8$ mm.

The objective of the investigation was to analyze the effect of particle size, concentration and average relative velocities on the collision rate between particles. Therefore, the test section sought to reduce the effects of other phenomena such as fluid turbulence and wall roughness, whose effects might result in uncertainties, which would make it difficult to emphasize on the interparticle collisions. Thereby, the tests used relatively large spherical particles with sufficiently high inertia for the influence of turbulence to be negligible.

3.2. Image processing method

The collision rate is a function of the particle diameter, concentration and relative velocities between particles. The particle diameter was directly measured as 1.8 mm. All the effective sequential images obtained last nearly 10 s, among which every 1000 sequential images were grouped to stand for one definite average data such as particle number density, relative velocity and collision rate. So the time interval Δt is 0.4995 s. The methods for obtaining the other parameters are described in the following sections.

3.2.1. Collision number

Determination of the number of collisions was the most difficult part of the experiment, since there are no ready-made algorithms to count collisions. A manual count of the collision was chosen as the most accurate method. The imaging software, ACDSee (ACD Systems Ltd, version 4.0) was used to show the particle motion process, and could easily display sequential images at

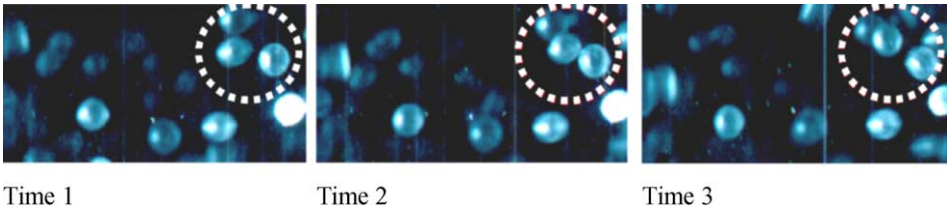

Fig. 5. Particle collision process.

various speeds. Fig. 5 shows a typical particle collision process, emphasized by the dashed circle in each image. The error was reduced by repeating the count several times until similar results were obtained for different counts.

3.2.2. Particle concentration

The particle concentration is the particle number per unit volume, which defined as $n = N_p/\Delta V$, where N_p is the number of particles in the investigation volume ΔV. An algorithm was developed to count the particles since a manual count would be too tedious. In the PTV technique, the first image-processing step is particle recognition (Raffel et al., 1998). An automatic threshold selection method (Otsu, 1980) was used to recognize the particles in the images. Fig. 6(b) shows the result of the particle recognition process for the image on the left. Fig. 6 shows that most particles in the visualized region were identified.

The visualized volume is based on the frontal area and the depth. The frontal area was measured using graph paper to get the size represented by each pixel in the images. The frontal area of the visualized volume was found to be $S = 18 \times 10^{-3} \times 8.5 \times 10^{-3}$ m^2 $= 1.53 \times 10^{-4}$ m^2.

The depth of the visualized volume could be measured directly by measuring the width of the laser sheet, which would be the depth of the visualized volume. But, the particles in the experiment were made of glass, which reflects light in all direction. Therefore, particles near the laser sheet would also be visible, so the real depth of the visualized volume was larger than the laser sheet width. A more accurate method was developed to measure the visualized volume depth. In the experimental setup shown in Fig. 7, a sloping surface with known incidence a was placed inside the test section with laser sheet entering from the side face, some of the particles used in the experiments were released from the top of the slope. Their movement from top to bottom was

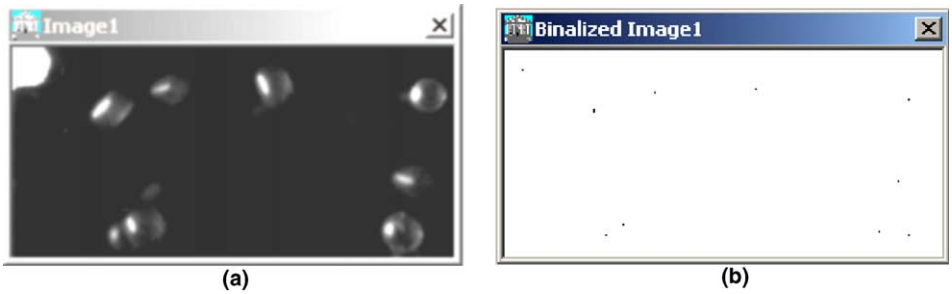

Fig. 6. Particle recognition for PTV technique: (a) original image, (b) recognition result.

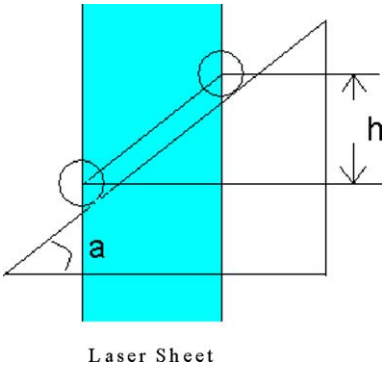

Fig. 7. Schematic diagram of method to measure laser sheet depth.

Fig. 8. Images for volume depth measurement (upper image shows particle entering the volume while the lower image shows the particle leaving the volume).

then recorded using a high-speed camera. The positions of the particles entering and leaving the field of view was measured by analyzing sequential frames to get the height, h, shown in Fig. 7. The visualized volume depth was then calculated from the geometry as $h/\tan(a)$.

Fig. 8 shows pictures of the particles entering and leaving the field of view at a camera speed 2000 fps. The image size was 256 pixel$\times$120 pixel with a corresponding real size of 36 mm$\times$17 mm. For the left particle in the images, the start position was (135,14) (pixels) while the final position was (122,96) (pixels). Therefore, $h = (96 - 14) \times 17/120 = 11.6$ mm with a incidence $a = 53.75°$, the volume depth was $w = h/\tan(a) = 8.5$ mm, so the visualized volume $\Delta V = 1.3 \times 10^{-6}$ m^3.

3.3. Relative velocity

The relative velocities between particles appearing in all images were calculated by measuring each particle's velocity using PTV technique. Various PTV algorithms, BICC (Yamamoto et al.,

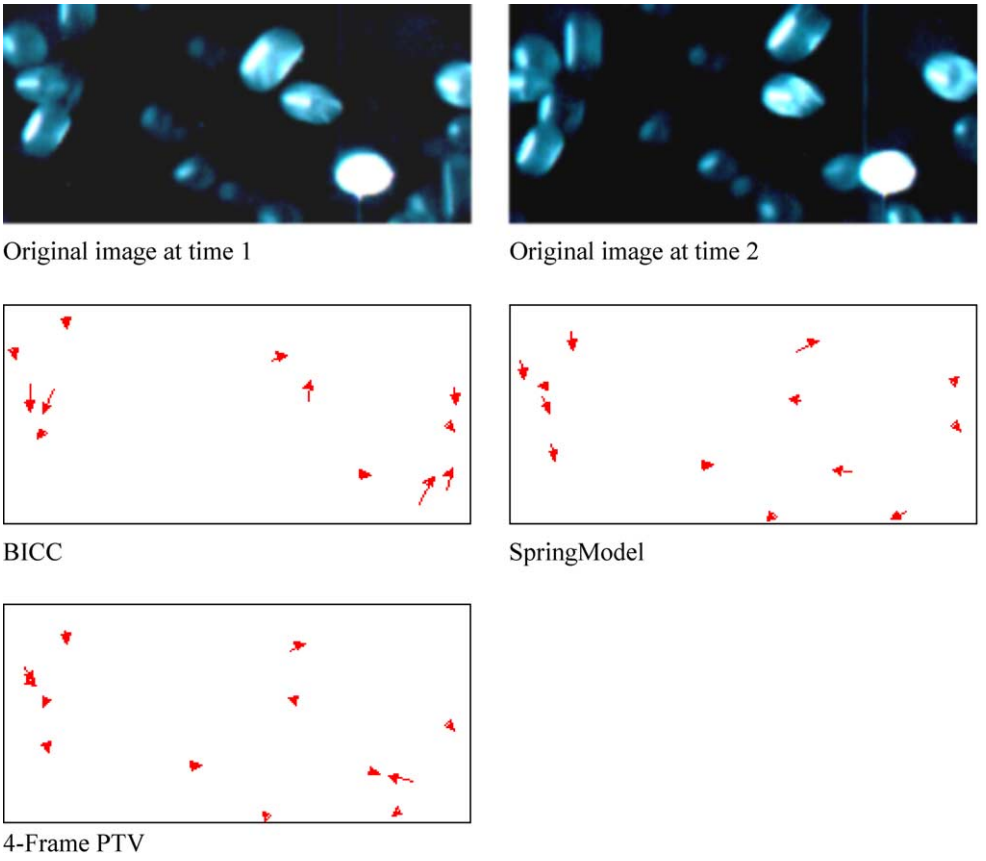

Fig. 9. Comparison of particle velocities calculated by different PTV algorithms.

1996), SpringModel (Okamoto et al., 1995) and 4-Frame PTV (Nishino and Torii, 1989) were evaluated with typical results given in Fig. 9. The automatic threshold selection method (Otsu, 1980) was used for the particle recognition in each image. Typical results from the automatic thresholds selection method are compared with a manual count in Table 1. The method for recognizing the particles in each image was always in good agreement with manual counts.

The results in Fig. 9 show that the SpringModel algorithm is better than the BICC and 4-Frame PTV methods, since it produces less spurious vectors. Table 2 compares the results from these algorithms and using manual pairing. The SpringModel had 82% accuracy. Therefore, SpringModel was used to pair the particles in the images to calculate the vectors for each particle.

Table 1
Comparison of a manual count and the automatic threshold selection method for particle recognition in a image

	Manual method	Automatic threshold selection method
Particles recognized	16	15

Table 2
Comparison between manual method and three PTV algorithms for pairing particles in two sequential images

	Manual	BICC	SpringModel	4-Frame
Total vectors	16	12	13	12
Exact vectors		11	13	11
Spurious vectors		1	0	1
Accuracy		69%	82%	69%

The relative particle velocities were based on the environmental particle concept in Eq. (11) and were calculated from the velocities of each particle in the volume. The velocity V_0 in Eq. (11) was calculated by averaging the velocity of the particles around the particle under consideration. Then, Eq. (11) was rewritten as:

$$\overline{v_{\mathrm{r}}} = \frac{1}{N_{\mathrm{p}}} \sum_{i=1}^{N_{\mathrm{p}}} \left(\frac{1}{N_{\mathrm{p}} - 1} \sum_{\substack{j=1 \\ j \neq 1}}^{N_{\mathrm{p}}} |\overrightarrow{v_i} - \overrightarrow{v_j}| \right) \tag{21}$$

Considering the difficulty in measuring three-dimensional velocity, we confined this experiments and analysis into a two-dimensional condition under the assumption that particles only moved in the investigation plane without the third velocity component in the spanwise direction affecting the particle collisions. And the experimental configuration was made to support this to some degree. The flow is two-dimensional at the beginning as the particles fall from the particle feeder. However, when the particles enter the convergent region, the third velocity component is no longer negligible, because the particles are not ideal spheres and the glass is not absolutely smooth. Further precise measurements are needed to make a three-dimensional analysis.

4. Experimental results and analysis

The theoretical expressions for particle collision rate, i.e. Eqs. (13) and (19), in gas-particle two-phase flow were validated by experimental data. The particle number density n, average relative velocity $\overline{v_{\mathrm{r}}}$, granular temperature Θ, particle diameter d and the total collision number C in the investigation volume ΔV and time interval Δt were measured directly. The experimental collision rate N_{c} is obtained by Eq. (20). Then they can be compared with the theoretical values calculated by Eqs. (13) and (19), and used to validate the theoretical expressions.

4.1. Effect of particle concentration and relative speed on collision rate

One class of particles with the diameter around 1.8 mm were used in the experiment, and the particle number density in the experiment was around $5\times10^6/\mathrm{m}^3$ with the volume fraction around 0.015. The average relative velocity was around 1.4 m/s. The camera speed was 2000 fps with the investigation area of 18 mm$\times$8.5 mm. Every 1000 sequential images were grouped to stand for

one definite average data such as particle number density, relative velocity and collision rate, so the time interval Δt is 0.4995 s.

Fig. 10 compares the experimental results of collision rate with the prediction of Eq. (13) with $\alpha = 1$. The results are obviously different in that the values of Eq. (13) are much higher than those of experimental results. Keeping the particle diameter constant, the collision rate calculated by Eq. (13) is proportional to $n^2\overline{v_r}$. While the experimentally determined collision rate is far from proportional to it. The least square fit by the function $y = ax^b$ shows that experimental collision rate is proportional to $(n^2\overline{v_r})^{0.547}$ in the investigation range of $1.96 \times 10^{13} \leqslant n^2\overline{v_r} \leqslant 5.62 \times 10^{13}$. Therefore, the expression obtained from kinetic theory does not accurately predict the collision rate in real gas-particle two-phase flow on a millisecond time scale and a millimeter space scale, i.e. the particle scale (1.8 mm in diameter).

If we assume that collision rate is proportional to average relative velocity, we can find the relation between collision rate and particle number density by least square fit. In the experiment the average relative velocities were keep nearly steady around a value of 1.4 m/s with only very small varieties. For more accurate data fit, each data of collision rate was divided by the relevant average relative velocity, and the function of $\frac{N_c}{\overline{v_r}}$ with particle number density n is fit according to the function form $y = ax^b$, which is shown in Fig. 11. This function is fit as:

$$\frac{N_c}{\overline{v_r}} = 0.842n^{1.15} \tag{22}$$

Therefore, the collision rate can be expressed as:

$$N_c = 0.842n^{1.15}\overline{v_r} \tag{23}$$

Considering the fixed particle diameter $d = 1.8$ mm, the general expression of collision rate can be rewritten in the form as Eq. (13) as:

$$N_c = 2.60 \times 10^5 d^2 n^{1.15}\overline{v_r} \tag{24}$$

It is shown that the experimental expression of collision rate is proportional to $n^{1.15}$, instead of n^2 as given by theoretical derivation. This result is reliable in the experimental condition with particle

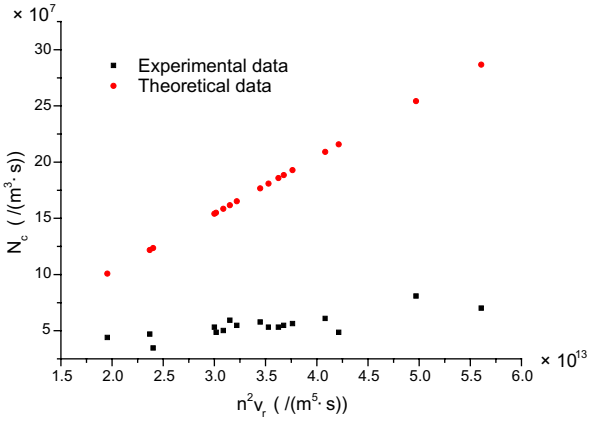

Fig. 10. Comparison of the collision rate determined experimentally with Eq. (13) with $\alpha = 1$.

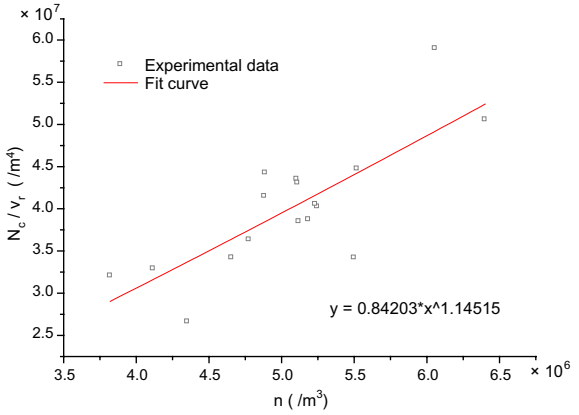

Fig. 11. Correlation fit of experimental collision results.

number density in the order of 10^6. And experimental data in more wide range of parameters is needed for confirmation. The experimental and theoretical expressions of collision rate are compared in Fig. 12. It is shown that collision rate of theoretical estimation is much higher than experimental curve when particle number density is higher than 1.27×10^6 and lower than experimental curve when particle number density is lower than this value. It means that at high particle concentration theoretical expression much overestimates the interparticle collision rate.

For this big difference between theoretical and experimental expressions, several reasons in the following may be responsible:

(1) The derivation of Eq. (13) is based on the kinetic theory of gases, especially, that the relative velocities between all the particles are nearly constant during the time interval Δt and particle i can collide with all other particles in the collision cylinder $\pi d^2|\overrightarrow{v_r}|\Delta t$ as shown in Fig. (2). But in the real conditions, the relative velocities and particle positions change dramatically when one particle collides with another particle. Therefore, during the time interval Δt, the relative

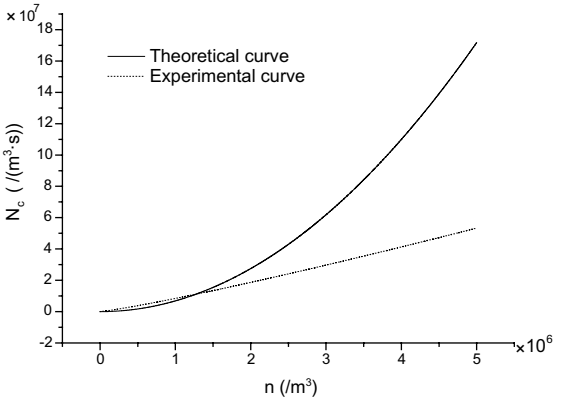

Fig. 12. Comparison of collision rate determined theoretically and experimentally.

velocities are not constant and particle i cannot collide with all particles in the collision cylinder for most cases. This assumption can cause the theoretical expression overestimate the collision rate in real particulate system. Eq. (13) may give more accurate results when the time step Δt is very small.

(2) Measurement errors may lead to some discrepancies between our results and those based on kinetic theory. In these tests, five parameters were measured, i.e. particle diameter, particle numbers in the images of investigation area, the visualized investigation volume, the total collision numbers and average relative velocities. Among these parameters, the last one, i.e. the relative velocity, was most difficult to accurately measure, since the flow is three-dimensional rather than two-dimensional. This analysis neglected the third velocity component parallel to the CCD lens, which should be very small. Additional measurements were taken with the vertical channel turned 90° and the CCD camera recording the particle motion in the third direction. The velocities ranged from 0 to 0.2 m/s, which is less than the other two velocity components in the plane of the laser sheet (about 4 m/s). Even this third velocity component is considered in the collision rate, the conclusion is still essentially the same, since there is a large difference between the experimental results for the collision rate and Eq. (13).

(3) The collision rate is shown not to be proportional to the square of the particle number density. But this experimental result still needs confirmation by more precise measurements in wider parameter range in the next stage.

4.2. Effect of granular temperature on collision rate

In our measurements, the granular temperature given by Eq. (16) can be written as:

$$\Theta = \frac{1}{3N_{\mathrm{p}}} \sum_{i=1}^{N_{\mathrm{p}}} |\overrightarrow{v_i} - \vec{u}|^2 \tag{25}$$

where $\overrightarrow{v_i}$ is the instantaneous velocity of particle i and $\vec{u}$ is the mean velocity:

$$\vec{u} = \frac{1}{N_{\mathrm{p}}} \sum_{i=1}^{N_{\mathrm{p}}} \overrightarrow{v_i} \tag{26}$$

The comparison of collision rate determined experimentally and theoretically by Eq. (19) is shown in Fig. 13. Similarly, the collision rate of theoretical estimation by Eq. (19) is obviously much higher than that determined experimentally. The theoretical estimation by Eq. (19) also much overestimates the collision rate in real particulate system.

4.3. Error analysis of three-dimensional flow

As pointed before, even if we initially had a strictly two-dimensional flow configuration at the upper part of the duct, collisions between particles always would remain a three-dimensional phenomenon. Especially in the collision region, the effect of the velocity normal to the plane of visualization is not negligible. But it is very difficult to make three-dimensional measurements in such a collisional flow by PTV technique. However an estimation of this error is significant.

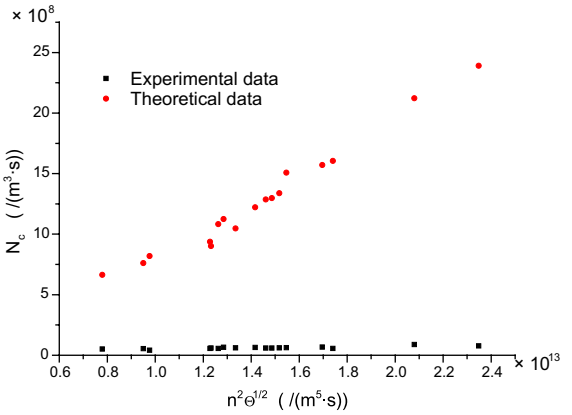

Fig. 13. Comparison of collision rate determined experimentally and by Eq. (19).

The CCD camera was transferred 90° to measure the third-dimensional velocity. It gave a rough estimation that the magnitude of the third-dimensional velocity was nearly 10–20% of that of the velocity in the investigation plane. On the other hand, because the flow configuration in this experiment was the same with that used by Fohanno and Oesterle's (2000) and the experimental conditions were similar, we can refer to the data supplied by them. Their measurement data showed that the velocity magnitude in the plane of visualization decreased 14% when progressing downwards the channel. The momentum transfer towards the normal direction by particle collisions was believed to contribute to this. So we can estimate that the magnitude of the velocity normal to the visualized plane is fewer than 20% of that in the plane. As for the relative velocity, this estimation is also credible. Considering that the big difference between the theoretical and experimental collision rate, we are sure that the qualitative collusion still holds, i.e. the theoretical expressions overestimate the collision rate. However, the fit expression from experimental data maybe relatively rough. More precise measurements are needed in the future work to obtain accurate collision models.

5. Conclusions

A high-speed CCD camera and advanced PTV algorithms were used to experimentally investigate interparticle collisions, especially the collision rate, on a millisecond time scale and a millimeter space scale, which is the particle size. The tests studied the relationship between interparticle collision rate, particle number density and average relative velocity, and compared the collision rate determined experimentally with that calculated by the expressions based on kinetic theory of gases. The experimentally determined collision rate was found to be much lower than predicted by the theoretical calculation, which means that the theoretical expressions overestimate the collision rate. Analysis of the experimental data led to a new correlation for more accurately predicting the collision rate for use in numerical simulations and theoretical analyses of gas–solid flows.

Finally, since the experimentally determined correlations of the collision rate for gas-particle two-phase flows differ greatly from the commonly used correlations based on kinetic theory, more experimental data are needed for further validation of the present conclusions in a full range of conditions to completely understand this problem.

Acknowledgements

The research was supported by the Special Funds for Major State Basic Research Projects (No. G19990222082). The authors would like to thank Prof. Fujio Yamamoto (Dept. of Mechanical Engineering, Fukui University, Japan) for providing the PTV programs and many helpful discussions.

References

Bird, G.A., 1994. Molecular Gas Dynamics and the Direct Simulation of Gas Flows. Clarendon Press, Oxford.

Carlos, C.R., Richardson, J.F., 1968. Solids movement in liquid fluidized beds. I: Particle velocity distribution. Chem. Eng. Sci. 23, 813–824.

Crowe, C.T., 1981. On the relative importance of particle–particle collisions in gas-particle flows. In: Proceedings of the Conference on Gas Borne Particles, Paper C78/81, pp. 135–137.

Fohanno, S., Oesterle, B., 2000. Analysis of the effect of collisions on the gravitational motion of large particles in a vertical duct. Int. J. Multiphase Flow 26, 267–292.

Gidaspow, D., 1994. Multiphase Flow and Fluidization: Continuum and Kinetic Theory Descriptions. Academic Press, Boston.

Matsumoto, S., Saito, S., 1970a. On the mechanism of suspension of particles in horizontal pneumatic conveying Monte Carlo simulation based on the irregular bouncing model. J. Chem. Eng. Japan 3, 83–92.

Matsumoto, S., Saito, S., 1970b. Monte Carlo simulation of horizontal pneumatic conveying based on the rough wall model. J. Chem. Eng. Japan 3, 223–230.

Nishino, K., Torii, K., 1989. A fluid-dynamically optimum particle tracking method for 2-D PTV: triple pattern matching algorithm. Transport Phenomena in Thermal Engineering, pp. 1411–1416.

Oesterle, B., Petitjean, A., 1991. Simulation of particle-to-particle interactions in gas–solid flows. In: Proceedings of the 1st International Conference on Multiphase Flows (ICMF'91), Tsukuba, Japan, 1, pp. 91–94.

Oesterle, B., Petitjean, A., 1993. Simulation of particle-to-particle interactions in gas–solid flows. Int. J. Multiphase Flow 19, 199–211.

Okamoto, K., Schmidl, W.D., Hassan, Y.A., 1995. Least force technique for the particle tracking algorithm. In: Proceedings of the 1st International Workshop on PIV'95-Fukui, p. 21.

Ottjes, J.A., 1978. Digital simulation of pneumatic particle transport. Chem. Eng. Sci. 33, 783–786.

Otsu, N., 1980. An automatic threshold selection method based on discriminate and least squares criteria. Denshi Tsushin Gakkai Ronbunsyuu (Japanese Proceedings), J63-D, No. 2, 349.

Pearson, H.J., Valioulis, I.A., List, E.J., 1984. Monte Carlo simulation of coagulation in discrete particle-size distribution. J. Fluid Mech. 143, 367–385.

Raffel, M., Willert, C.E., Kompenhans, J., 1998. Particle Image Velocimetry. Springer-Verlag, Berlin, Heidelberg, Germany.

Sommerfeld, M., 1994. The importance of detailed measurements for the validation of numerical models and methods for dispersed two-phase flows. In: Celik, I. et al. (Eds.), Experimental and Computational Aspects of Validation of Multiphase Flow CFD Codes, FED-vol. 180. ASME, Washington, DC, pp. 1–14.

Sommerfeld, M., 1995. The importance of inter-particle collisions in horizontal gas–solid channel flows. In: Stock, D.E. et al. (Eds.), Gas-Particle Flows, FED-vol. 228. ASME, pp. 335–345.

Sommerfeld, M., 2001. Validation of a stochastic Lagrangian modeling approach for inter-particle collisions in homogeneous isotropic turbulence. Int. J. Multiphase Flow 27, 1829–1858.

Sommerfeld, M., Zivkovic, G., 1992. Recent advances in the numerical simulation of pneumatic conveying through pipe system. In: Hirsch et al. (Eds.), Computational Methods in Applied Science First European Computational Fluid Dynamics, Brussels, pp. 201–212.

Sundaram, S., Collins, L.R., 1997. Collision statistics in an isotropic particle-laden turbulent suspension. Part 1. Direct numerical simulations. J. Fluid Mech. 335, 75–109.

Tanaka, T., Tsuji, Y., 1991. Numerical simulation of gas–solid two-phase flow in a vertical pipe: on the effect of inter-particle collision. In: Stock, D.E. et al. (Eds.), Gas–Solid Flows, 1991, FED-vol. 121. ASME, pp. 123–128.

Tsuji, Y., Tanaka, T., Ishida, T., 1990. Graphic simulation of plug conveying. In: Proc. Pneumatech 4, Glasgow, Scotland, pp. 39–50.

Williams, J.J.E., Crane, R.I., 1983. Particle collision rate in turbulent flow. Int. J. Multiphase Flow 9, 421–435.

Yamamoto, F., Wada, A., Iguchi, M., Ishikawa, M., 1996. Discussion of the cross-correlation methods for PIV. J. Flow Visualization Image Process. 3, 65–78.